334 *Macromolecules* **2010**, *43*, 334–346
DOI: 10.1021/ma901999j

Macromolecules
ARTICLE

Novel Experimental Approach To Evaluate Filler−Elastomer Interactions

J. L. Valentín,*,†,‡ I. Mora-Barrantes,† J. Carretero-González,† M. A. López-Manchado,† P. Sotta,§ D. R. Long,§ and K. Saalwächter*,‡

†*Institute of Polymer Science and Technology (CSIC), C/Juan de la Cierva 3, 28006 Madrid, Spain,* ‡*Martin-Luther-Universität Halle-Wittenberg, Institut für Physik−NMR, Betty-Heimann-Str. 7, D-06120 Halle, Germany, and* §*Laboratoire Polymeres et Matériaux Avancés, CNRS/Rhodia. 85 avenue des Freres Perret, F-69192 Saint-Fons, France*

Received September 7, 2009; Revised Manuscript Received October 28, 2009

ABSTRACT: Novel information on filler−elastomer interactions is obtained by combining solid-state ^{1}H low-field NMR spectroscopy and equilibrium swelling experiments. Multiple-quantum (MQ) NMR experiments provide detailed quantitative molecular information on the cross-link density of the elastomer matrix in a variety of filled systems, indicating generally weak filler effects on the overall cross-link density and on the network homogeneity. Swelling experiments, as well as mechanical data, are additionally influenced by the matrix−filler and filler−filler interactions. Our approach is based on comparing cross-link densities from NMR and (Flory−Rehner) swelling experiments, for which a *masterline* is always found in unfilled elastomers. In filled elastomers two different scenarios are observed. If there are no interactions between the polymer chains and the filler surface, no deviations from the masterline are detected because the swelling capacity of the composite is governed by the bulk polymer. Deviations from the masterline (reduced swelling) are exhibited by those composites that have strong rubber−filler interactions. In these cases, some fraction of the polymer is connected to the filler surface, which thus behaves like a giant cross-link, and the overall degree of swelling is thus reduced as compared to the bulk polymer. The novel experimental approach was used to evaluate filler−elastomer interactions in different composites and nanocomposites.

Introduction

Elastomers are important polymeric materials because of their unique elastic properties. However, the reinforcement of these soft matrices is essential to realize the required properties for the many different practical applications.[1−4] Fillers are extensively used in the rubber industry, not only to reinforce the polymer matrix but also to improve the rubber processing and, in some cases, to reduce the price of the final material. In this sense, rubber reinforcement can be considered as one of the most important topics in rubber science and technology.

Carbon black is the most widely used filler in rubber technology.[5−7] In addition to reinforcing effects caused by the fractal nature of both carbon black aggregates and larger-scale filler networks in the rubber matrix,[8−10] the surface activity[11] plays a key role in controlling the polymer−filler interactions and therefore the overall reinforcement. Today, carbon black is increasingly substituted by cheaper and more environmentally friendly inorganic particles[12,13] such as silica.[14−17] Contrary to carbon black, inorganic fillers have a much reduced affinity toward the elastomer components and thus tend to form large aggregates, leading to drawbacks in processing and poor reinforcement.[17] These problems are usually overcome by surface modification of these fillers with bifunctional organic molecules[18,19] improving the interaction with the elastomer and therefore enhancing the reinforcement effect.[20,21]

Elastomer *nano*composites represent one step forward in this field,[22−26] as they hold promise for properties that cannot be realized with their microcomposite counterparts.[27,28] The qualitative difference is caused by distinct characteristics[29,30] arising from the nanoscopic dimensions and high aspect ratio of the nanofillers, such as a low percolation threshold, a large interfacial area, and potential confinement effects on the polymer properties. However, it is important to remark that the final properties are still short of the idealized theoretical predictions,[31,32] i.e., the much-desired *nano*effect. This discrepancy arises from imperfect dispersion of the filler and poor load transfer from polymer matrix to the nanoparticle,[31,32] calling for optimization and corresponding analytical tools.

It is clear that reinforcement of elastomers, or more general polymers, by addition of particles or nanoparticles is a complex phenomenon that depends on several factors.[33] In most simple terms, the final properties of the composite are primarily dictated by the addition of inherent properties of the different components that constitute the material, i.e., the so-called hydrodynamic effect. In addition, the actual reinforcement is strongly affected by the arrangement of the particles that are often dispersed as fractal aggregates,[10] caused by the surface activity of the particles.[11] In addition, the fractal structure undergoes characteristic changes on straining the samples, modifying the reinforcing effect.

The other central factor that determines the variation of the bulk properties in filled polymers is related to the particle−polymer interface. Polymer chains that interact with the particle surface suffer a substantial modification of their chain dynamics, for instance, leading to shifts of the glass transition temperature (T_g).[17,34−38] The existence of a glassy layer (interface) has been established by different experimental techniques,[36−40] and it is consistent with the effect of polymer−substrate interaction on T_g observed in thin films.[41−46] Assuming a gradient of the glass transition temperature away from the particle interface,[47−50] a mesoscale model to explain the reinforcement of elastomers in

*Corresponding authors. E-mail: jlvalentin@ictp.csic.es (J.L.V.); kay.saalwaechter@physik.uni-halle.de (K.S.).

 Published on Web 11/16/2009

Table 1. Summary of the Studied Sample Series and Their Composition Permutations

sample series	optional filler (phr)[a]	optional coupling/modification agents A−D (phr)[a]
NR1-50S-A	silica (50)	TESPT (4)
NR2-45CB	carbon black (45)	
NR3-xxS-A,B,C	silica (10; 20; 30; 40; 50; 60)	TESPT (1; 2; 3; 4; 5; 6); MS (4); NXT (4)
NR4-10Clay-D	clay (10)	ODA (∼2.8)
NR5-u-D		ODA (2.8)
NR6-xFGS	TEGO (1; 1.5; 4)	
NR6-1.5LSFGS	low-surface TEGO (1.5)	
NR6-16CB	carbon black (16)	
SBR1-50S-A	silica (50)	TESPT (4)
SBR2-45CB	carbon black (45)	
SBR3-40S-A,B,C	silica (40)	TESPT (4), MS (4), NXT (4)

[a] The numbers in parentheses indicate the amount of each ingredient in parts per hundred of rubber (phr). Note that in the NR3 series the silane content (A, B, or C) is adjusted according to the silica content.

both the linear and nonlinear regimes (Payne and Mullins effects) has been developed.[51] According to this model, the glassy layer around the particles (or aggregates) is responsible for the reinforcement because it acts as a "glue" between the particles, rendering its effect particularly strong when combined with a percolation of the filler network.[51] This scenario provides a natural explanation of the differences between conventional (micro-) and nanocomposites, where the former have comparably less interphase and exhibit significant reinforcement only at higher volume fraction of filler. Nanocomposites exhibit a larger relative interphase volume, and percolation occurs at much lower volume fraction, with correspondingly large effects on the bulk properties.[52−54]

The main problem at this point is the insufficient information about structure−properties relationships (mainly in the nanocomposites field), caused by the lack of experimental procedures to obtain quantitative or at least semiquantitative information about the behavior of the interface.[55,56] In this sense, solid-state NMR is one of the most useful and successful tools to investigate the filler−rubber interactions by measuring the additional topological constraints arising at the filler surface.[57−64] The central NMR observable is the residual dipolar couplings (D_{res}), characterizing local chain order arising from nonisotropic fast segmental motions of the polymer chains, which in turn arise from constraints to the chain motion. These constraints are imposed by entanglements or absorption/proximity to fillers (physical constraints) or by cross-links or polymer filler bonds (chemical constraints). Many NMR experimental procedures have been used to estimate D_{res},[65−69] but Hahn and solid echo relaxometry experiments (usually performed in low-field spectrometers) are the most used procedures to study the interface in filled elastomers.[57−61] However, it is important to point out that such data must be analyzed very carefully, since the results can be incorrect when the data are overinterpreted.[60−72] For instance, recent work of our group[71,73] indicated that in a series of styrene−butadiene (SBR) rubber compounds filled with carbon black and silane-modified silica, in contrast to the significant influence of filler particles on the average cross-link density observed by transverse relaxometry experiments,[74] multiple-quantum NMR experiments revealed only insignificant variations of the average state of order (directly related to the cross-link density of the actual matrix polymer) in those compounds. This was explained by the fact that Hahn-echo (T_2) relaxometry is subject to nondipolar effects; thus subsequent fits produced artifacts.[71] Therefore, we consider double-quantum (DQ) or, more generally, multiple-quantum (MQ) NMR as the best method for the measurement of weak residual dipolar couplings in composites.

In this work, the structures of series of natural rubber (NR) and SBR compounds filled with conventional (micrometer-sized) particles as well as different types of nanoparticles are investigated by MQ experiments performed on low-field NMR spectrometers. As noted, the swelling behavior of rubber compounds is determined not only by the polymer network structure,[75] but it is also restricted by the boundary conditions at the surface of the particles.[76] In this article, by combining MQ NMR and equilibrium swelling experiments in filled rubber compounds, we investigate the nature of the filler−rubber interface, taking as a reference the elastomer bulk behavior. In addition, elastomer nanocomposites will be studied in detail in order to obtain some evidence on the origin of their exceptional improvement of properties in comparison with the conventional composites.

Experimental Section

Materials and Preparation of Samples. Standardized natural rubber (NR) and styrene−butadiene (SBR) rubbers filled with different microparticles and nanoparticles were prepared using standard procedures. Table 1 shows a brief summary of the analyzed samples. More detailed descriptions of the sample recipes and preparation procedures are provided as Supporting Information.

Samples used to analyze the swelling behavior of unfilled NR were described in another recent article[75] (not listed in Table 1). The aim of this sample series is to cover the range of cross-link densities used for practical uses in rubber technology with the most useful cure systems, i.e., sulfur-based cure systems (conventional and efficient according to the accelerant/sulfur ratio) and a peroxide cure system (dicumyl peroxide). These samples produce a *masterline* in a plot of the NMR-determined cross-link density vs the swelling-derived cross-link density.[75]

In order to obtain a similar *masterline* for SBR compounds, a series of SBR samples were vulcanized with a conventional vulcanization system with increasing sulfur content. All unfilled compounds are generally denoted with "u" and are not explicitly listed in Table 1, e.g., NR1-u and SBR1-u. They were always prepared following the same recipes as the filled conterparts. Two series of NR and SBR compounds were filled with a constant volume fraction of precipitated silica (NR1, SBR1) and carbon black (NR2, SBR2). The NR1-50S-A and SBR1-50S-A compounds were filled with silica (50 phr) and additionally contain 4 phr of bis(triethoxysilylpropyl)tetrasulfane (TESPT) as coupling agent.

The NR3 and SBR3 series are also filled, but with varying contents of modified silica. These composites were prepared in order to study the influence of both the content of filler and the chemical structure of the coupling agents on the swelling capacity of the material. In these cases, the silica surface was modified (before the addition to rubber compound) with diethylene glycol (DEG) and three different silanes: TESPT, mercaptopropyltrimethoxysilane (MS), and 3-octanoylthio-1-propyltriethoxysilane (NXT). To study the influence of DEG and the different coupling agents on the vulcanization process, a series of unfilled samples were prepared by adding just DEG (NR3-u; SBR3-u) and additionally the corresponding silane (NR3-u-A.B,C, SBR3-u-A,B,C).

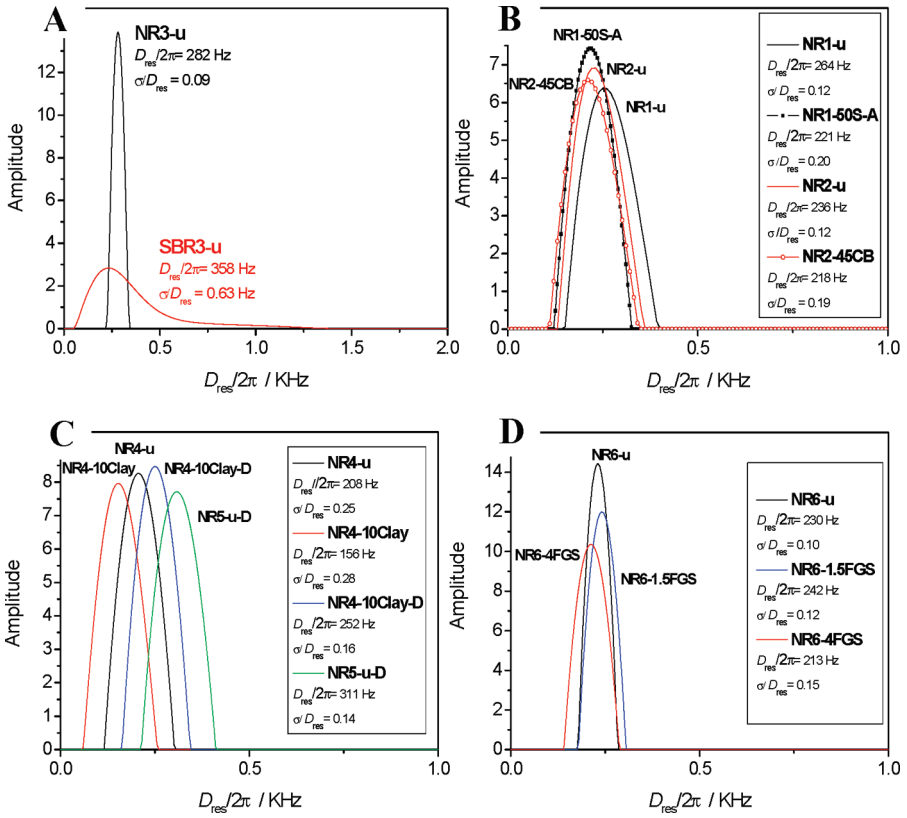

Figure 1. Distribution of residual dipolar couplings obtained by numerical analysis of I_{nDQ} via Tikhonov regularization. Unfilled NR and SBR samples in (A) have the same recipe. Addition of silica or carbon black (B), clay or organo-clay (C), or different amounts of graphene (D) do not lead to any remarkable change in the cross-link distribution with respect their unfilled counterparts. The shift of the maxima to higher values in (C) is related with the efficiency of the vulcanization reaction. Amines used to modify clay particles act as accelerators, increasing the efficiency of the vulcanization reaction (see below).

Generally, the names of the compounds, e.g., NR3-40S-A, contain the type of rubber (NR or SBR), the recipe index (3), the amount of filler (40 phr) and its type (S = silica), and the modifier molecule (A = TESPT, B = MS, C = NXT).

NR−clay nanocomposites with a sulfur-based cure system were prepared following recipes published elsewhere.[27] The NR4-10Clay samples contain different amounts of the cure system and 10 phr of pristine montmorillonite (MMT). NR4-10Clay-D samples include 10 phr of MMT modified with octadecylamine (ODA). NR5-u-D samples do not contain any filler but additionally have 2.8 phr of ODA to evaluate the effect of ODA in the vulcanization reaction. For more details on the clay structure and the clay modification see ref 27.

The NR6 samples are graphene-based nanocomposites featuring different contents (1−4 phr) of functionalized graphene sheets (FGS), also referred to as "thermally expanded graphite oxide" (TEGO), as described in ref 77. In addition, two compounds contain 1.5 and 16 phr of low surface FGS and carbon black, respectively. All samples were prepared by a solution processing technique.[77] Details on the preparation and characteristics of FGS were published elsewhere.[78]

Most specimen were cured in a laboratory press at 150 °C (160 °C for SBR series 1 and 2) at their respective optimum times, i.e., t_{95} or t_{97}, according to the rheometer curves.

Determination of M_c by Equilibrium Swelling. The average mass of network chains between cross-links (M_c) was determined by equilibrium swelling experiments, taking into consideration all the recommendations given in our previous work.[75] M_c was calculated based on Flory−Rehner theory, assuming a phantom model to describe the elastic behavior of the swollen network (pointing out that this is merely an assumption validated by better agreement with NMR results;[81] experimental proof unambiguously identifying the better applicability of the affine vs the phantom model is still lacking). The rubber density, ρ_r, was measured via the hydrostatic weighing method.[75] Toluene was the solvent in these experiments; therefore, the molar volume and density of the solvent were taken as $V_s = 106.2$ mL/mol and $\rho_s = 0.87$ g/cm^3, respectively.

To calculate the volumetric fraction of rubber, five weighed test pieces of rubber (pieces of approximately 6 mm diameter and 2 mm thickness were used), w_i, were immersed in toluene at 22 °C for a period of 24 h in sealed dark vials, in order to protect the swollen sample from light. As was demonstrated previously,[75] these measures ensure that swelling equilibrium is reached and that the sample degradation is minimized. Then, the samples were blotted with tissue paper to remove the excess of the solvent and immediately weighed on an analytical balance with an accuracy of ~10^{-5} g (w_s). Finally, the samples were dried in a vacuum oven for ~24 h at 60 °C until constant weight (w_d), and eq 1 was used to determine the rubber fraction, ϕ_r:

$$\phi_r = \frac{\dfrac{w_d - f_{ins} w_i}{\rho_r}}{\dfrac{w_d - f_{ins} w_i}{\rho_r} + \dfrac{w_0^{sol}}{\rho_s}} \quad (1)$$

Here, f_{ins} is the weight fraction of insoluble components, which depends on the sample recipe, and w_0^{sol} is the equilibrium weight of the swelling solvent. In this work, zinc oxide and filler particles were considered to be insoluble components. These particles do not swell and have to be subtracted in order to obtain the actual rubber fraction. According to the experimental procedure described previously, without sample degradation effects it is possible to accurately determine this parameter as the weight of liquid taken up after 24 h ($w_{24\,h}^{sol}$): $w_0^{sol} = w_{24\,h}^{sol} = w_s - w_d$. The given rubber volume fractions are always the average over five test pieces per sample.

However, eq 1 does not take into consideration the excess of solvent placed in the vacuole formed around particles with no interactions with the rubber. This effect plays an important role in filled compounds; therefore, in samples without rubber−particle interactions, the excess solvent has to be taken into account as follows:[75]

$$\phi_r = \frac{1 + \dfrac{(f_{ins} w_i)/\rho_{ins}}{(w_d - (f_{ins} w_i))/\rho_r}}{\dfrac{\dfrac{w_d - f_{ins} w_i}{\rho_r} + \dfrac{w_0^{sol}}{\rho_s}}{\dfrac{w_d - f_{ins} w_i}{\rho_r}} + \dfrac{(f_{ins} w_i)/\rho_{ins}}{(w_d - (f_{ins} w_i))/\rho_r}} \quad (2)$$

where ρ_{ins} is the density of the insoluble particles. Finally, it is important to use a correct value of the Flory−Huggins parameter χ, which in fact depends on the volumetric fraction of rubber[75] and is also different for networks vs linear polymers.[79,80] Taking this fact into consideration, we used the expression[81] $\chi = 0.427 + 0.112\phi_r^2$ for the NR−toluene pair. To the best of our knowledge the ϕ_r dependence of χ for the SBR−toluene pair was not studied yet with sufficient precision for the case of networks, which is why we use a constant value of $\chi = 0.413$.[82]

Determination of M_c by Proton NMR Spectroscopy. Proton MQ spectroscopy is probably the most versatile and robust quantitative technique to investigate not only the structure but also the dynamics of polymer networks, based on the determination of partially averaged residual dipolar coupling constants (D_{res}), given in units of rad/s.[69] The essential advantage of MQ spectroscopy as compared to more traditional NMR approaches such as Hahn or solid echoes is that, without invoking any specific model, effects of temperature-independent network structure and temperature-dependent chain dynamics can be quantitatively separated, in the high-temperature regime, as explained in much detail our previous papers.[69,72,83] The major trick is to analyze a so-called normalized DQ (nDQ) build-up curve, which is obtained by suitable processing of the experimental DQ build-up and reference decay curves, all curves being measured as a function of the double-quantum evolution time τ_{DQ} (= variable duration of the pulse sequence). We here only mention some experimental basics that are particularly relevant in the given context.

Experiments were carried out on a Bruker minispec mq20 spectrometer operating at 0.5 T with 90° pulses of 1.7 μs length and a dead time of 12 μs. It is important to note that the experimental result, D_{res}, is directly proportional to the (local) cross-link density and that possible distribution effects of D_{res} related to different end-to-end separations and polydispersity of network chains do not play any role in the case of natural rubber because of the cooperativity of the reorientational dynamics on the length scale of a few network chain lengths that averages the observable.[84] Therefore, the nDQ build-up curves could be analyzed in the quasi-static limit in terms of a single D_{res}. Distribution effects only come in when the sample has spatial variations in cross-link density that exceed the length scale of one or a few R_g.

However, the case of SBR samples is different in that styrene-*co*-butadiene rubber exhibits an apparently broader D_{res} distribution due to the different comonomers with different local coupling topologies. This point is best illustrated by results from a regularization analysis, providing direct access to the distribution function by numerical inversion,[83] using fast Tikhonov regularization.[85,86] This provides a qualitative picture of the distribution of residual couplings, and the differences among the samples can be appreciated in Figure 1. In part A, it is readily apparent that SBR features an intrinsically broader distribution. Results that are less prone to systematic errors related to experimental inaccuracies are obtained by fitting the experimental DQ build-up curves under the assumption of a Gaussian distribution of dipolar couplings[69]

$$I_{nDQ}(D_{res}, \sigma) = \frac{1}{2}\left(1 - \frac{\exp\left\{-\frac{\frac{2}{5}D_{res}^2\tau_{DQ}^2}{1+\frac{4}{5}\sigma^2\tau_{DQ}^2}\right\}}{\sqrt{1+\frac{4}{5}\sigma^2\tau_{DQ}^2}}\right) \quad (3)$$

which yields both an *average* apparent coupling constant and its standard deviation σ characterizing the distribution width. It is important to note that, contrary to NR compounds, due to the broader intrinsic distribution, most of the SBR samples are close to the limit of applicability of this fitting function, with σ being approximately half of the average D_{res}. At significantly larger σ, the distribution function would extend into the negative quadrant, imposing a systematic error on the average D_{res}. In the following, we always give σ in units of D_{res}. From Figure 1, it is obvious that the D_{res} distribution in all NR samples, and thus the overall heterogeneity in the cross-link density, is rather small ($\sigma/D_{res} < 1/4$), indicating no significant effect of any of the used fillers on the overall spatial heterogeneity in cross-link density.

In order to obtain a quantitative interpretation of the average molecular weight of network chain between cross-links, M_c, extracted from the NMR-determined D_{res}, it is necessary to define the "rigid-limit" coupling D_{stat}/k, taking into consideration a rescaling factor k that considers fast (∼picoseconds) dynamics inside the statistical (Kuhn) segments. The local dynamic order parameter of the polymer backbone[69] S_b, which is defined as a time average over the fluctuations of the segment-fixed dipolar tensor over the time until a plateau region is reached, is obtained as

$$S_b = k\frac{D_{res}}{D_{stat}} = \frac{3}{5}\frac{r^2}{N} \quad (4)$$

Equation 4 connects the experimental observable with the network parameters. The dimensionless factor r is the ratio of the end-to-end vector to its average unperturbed melt state ($r^2 = \mathbf{r}^2/\langle\mathbf{r}^2\rangle_0 = 1$ in unstrained rubbers), and N is the number of statistical segments between constrains. The last quantity can be converted into M_c via a calculation involving the characteristic ratio C_∞, noting that the cross-link density is $1/M_c \sim 1/N$.

From previous spin dynamics simulations, and assuming a reasonable model for the intrasegmental motions, an apparent reference coupling for natural rubber was obtained,[72] $D_{stat}/k = 2\pi \times 6300$ Hz. The final M_c is obtained as

$$M_c = \frac{617\ \text{Hz}}{D_{res}/2\pi}\ \text{kg/mol} \quad (5)$$

In SBR, the comonomer-specific D_{res} and the complex spin dynamics of the PS comonomer with its phenyl side group performing independent rotational jumps would require an in-depth analysis of the spin dynamics based on a suitable model for the local molecular dynamics, which was not yet done. We therefore refrain from converting the fitted D_{res} into actual values of cross-link density. Because of the perfect proportionality, we therefore simply take $D_{res} \sim 1/M_c$ as a measure of cross-link density.

Determination of Freezing Point Depression: Cryoporosimetry. The determination of the freezing point depression of solvent imbibed in rubber compounds (also termed cryoporosimetry) has been used not only to obtain (qualitative) information about the rubber network structure[87] but also to study filler−rubber interactions.[88] To perform these experiments, small pieces of rubber (around 5 mm^3) were swollen in cyclohexane (because of its favorable crystallization behavior in DSC), protecting the samples from the light in order to prevent

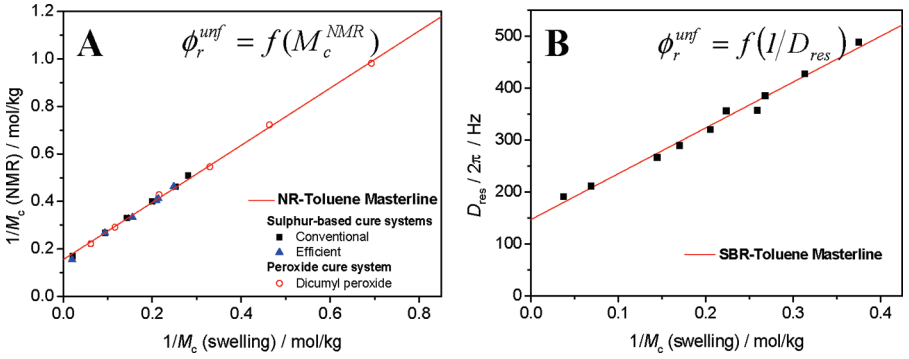

Figure 2. Comparison of swelling-determined reciprocal inter-cross-link molecular weights with corresponding results from NMR experiments for unfilled NR (A) and SBR (B) compounds. Note that a conversion factor for D_{res} into $1/M_c$ for the case of SBR is not yet available.

photo-oxidative degradation.[75] After 1 day, samples reach the swelling equilibrium and are placed in the DSC pans with some excess of solvent preventing deswelling by vaporization.

Freezing is a complex thermodynamic/kinetic process, in our case crucially influenced by the way a rubber network interferes with crystal nucleation. This is the reason why several authors prefer the measurement of melting point[89] rather than the freezing temperature to study the network structure. We note that in our case both experiments gave qualitatively the same information.

DSC experiments were carried out on a Mettler Toledo differential scanning calorimeter (DSC 822^e). All results for the liquid−solid or solid−liquid transition discussed in this work are mean values of at least three samples, with a cooling or heating rates of 5 °C/min, which represent the most favorable condition in order to obtain well-reproducible results.[87]

This experimental procedure is based on the anomalous melting point depression of the solvent imbibed in the elastomer compound caused by the finite and rather small crystal size, as a result of dimensional restrictions caused by the size of the three-dimensional polymer mesh. Therefore, the difference (ΔT) between the melting (or freezing) temperature of pure solvent (T_0) and the solvent that is imbibed in the rubber compound (T) is directly related to the dimensional restrictions imposed by the rubber network. In unfilled compounds, it is consequentially related to the cross-link density or $1/M_c$. In filled compounds, different scenarios are possible:[88] (i) without filler−elastomer interactions, a vacuole of pure solvent forms at the interface, whose size is related to the filler particle size, and within which the dimensional restrictions related to the rubber network are released; hence, a reduction in the freezing point depression is expected; (ii) with filler−elastomer interactions, leading to an interface containing a rubber fraction with equal or higher cross-link density as compared to the bulk network, the nucleation will mainly take place in the bulk network, and therefore ΔT should not vary much as compared to the corresponding unfilled sample; (iii) with the attached filler significantly reducing the overall swelling of the rubber network, the freezing point depression is increased. In consequence, this experiment gives important qualitative information on the elastomer composites.

Results and Discussion

The main goal of this paper is to obtain information on the filler−elastomer interface by combining apparent cross-link densities obtained by ^{1}H low-field solid-state NMR and equilibrium swelling experiments. It is important to note that the NMR results (taken on unswollen samples) are characteristic for the whole matrix polymer in all cases. The perfect linear correlation observed for unfilled elastomers represents the swelling behavior of the polymer *matrix*, and it only depends on the polymer−solvent pair. Taking these masterlines as reference, we evaluate the *swelling restrictions* caused by filler−elastomer interactions, which depend critically on the interface in the different systems. Our purpose is to provide an overview of the effects observed in the most common rubber micro- and nanocomposites. The work is structured as follows. First, we compare the interfaces of rubber compounds filled with silica and carbon black, which are the most important conventional fillers used in rubber technology. Second, we evaluate the influence of different coupling agents on the silica−elastomer interface, comparing samples with different filler content. Third, we show results for nanocomposites, taking rubber−clay nanocomposites as one of the most widely studied system in this field and finally focusing on a novel elastomer nanocomposite system based on functionalized graphene sheets (FGS).

Combining all these data, we arrive at a comprehensive picture of the different interface behaviors of the different filled elastomers, noting again that we only employ to-date standard experiments involving low-cost technology.

A. Unfilled Compounds. Swelling Masterlines. Different linear relationships are obtained when swelling results are compared with the NMR observable (Figure 2). Independently of the elastomer, NR or SBR, or cure system, the NMR/swelling correlation demonstrates that the scaling relationship $D_{res} \sim S_b \sim N^{-1} \sim M_c^{-1}$ assumed for the NMR analysis is correct. There are of course still uncertainties in the prefactors, related to the model assumptions involved in both experimental approaches,[75,84,90] yet important independent conclusions can be drawn.

First of all, it is important to note that the NMR experiment is sensitive to both physical (entanglements) and chemical (cross-links) constraints, and therefore it gives information on the *actual* number of elastically active network chains present in the dry sample. On the other hand, swelling of elastomer networks is a complex nonhomogeneous process, where excluded-volume effects, subaffine local deformation, and topological reorganization with a possible partial release of nontrapped entanglements ("desinterspersion") all play a role.[90−92] The y intercept in Figure 2 is in fact related to the entanglement contribution that is fully measured by NMR but is not fully active in restricting the overall swelling (only a part of the entanglements are topologically "trapped"), so the intercept is somewhat lower than $1/M_e$. In the case of NR, the obtained value at the y intercept gives 6450 g/mol, which is consistent with values already published for the entanglement molecular weight (6200 g/mol), obtained from rheology measurements.[93,94]

It is important to note that natural rubber networks (Figure 2A) exhibit the same linear relationship independently of the cure system (at least over the shown cross-link

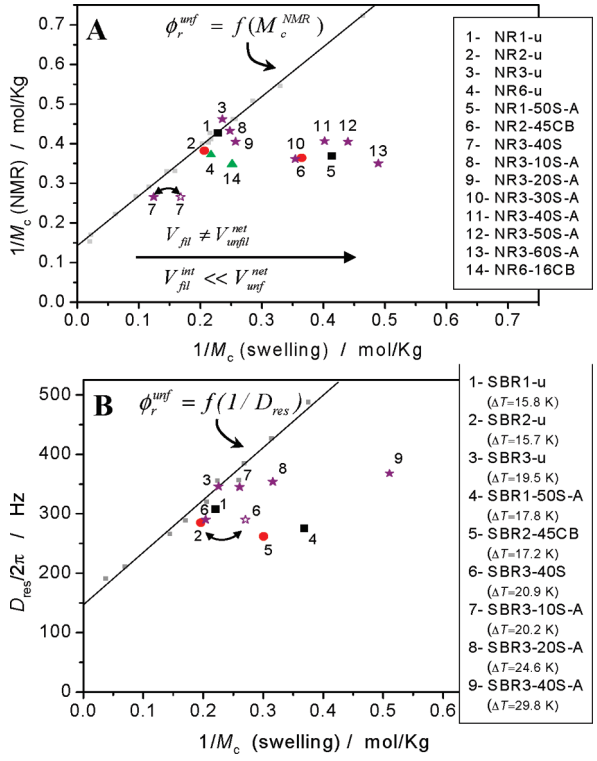

Figure 3. Representation of the true cross-link density (measured by NMR) as a function of $1/M_c$ derived from swelling for different series of conventional filled elastomers. Lines represent the swelling behavior of unfilled (bulk) NR (A) and SBR (B) networks. The double arrow highlights the correction effect on $1/M_c$ (swelling) when eq 2 (unfilled symbol) is used to eliminate the excess of solvent that eq 1 does not take into consideration (filled symbols). Bracketed values in the legend represent the freezing point depressions of cyclohexane imbibed in these samples.

density range), corroborating the independence of the extracted results from differences in the very local structure of these networks, i.e., the chemical nature of the cross-links, the cross-link distribution, and the amount of (elastically inactive) network defects (which are independently obtained by NMR and do show substantial variations that are the subject of an independent publication). We thus conclude that this type of representation characterizes the swelling behavior of the rubber matrix according to the specific polymer−solvent interaction parameter χ and the elastic answer of the bulk elastomer matrix.

The parameter χ is a complex quantity, being influenced by both entropic and heat of mixing terms, thus depending on the polymer−solvent pair and the volume fraction of rubber. The second contribution, i.e., the elastic answer of the network in swollen state, is obviously insensitive to the very local structure of the network, but it depends strongly on the number of elastically active junctions. The rubber fraction in swelling equilibrium ϕ_r is thus directly related to the cross-link density $1/M_c$ (or $1/D_{res}$ in the case of SBR) measured by NMR, $\phi_r^{unf} = f(M_c^{NMR})$. Figure 2B in fact proves that within the studied range of cross-link densities the neglected concentration effects on χ for SBR are not too large.

B. Filled Compounds. *1. Silica and Carbon Black Composites.* To investigate the importance of the interface of rubber compounds filled with the most commonly used fillers, e.g., silica and carbon black (with their micrometer-sized aggregates), their respective unfilled samples were taken as references. As it is expected, the swelling capacity

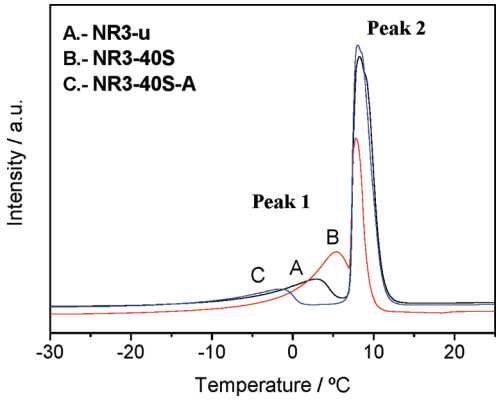

Figure 4. DSC heating curve of cyclohexane in swollen NR compound. Comparative melting point depression of unfilled NR (A) with those compounds filled with pristine silica (B) and TESPT-modified silica (C).

of the unfilled samples falls on the masterline, $\phi_r^{unf} = f(M_c^{NMR})$. Figure 3 confirms that ϕ_r^{unf} is mainly defined by the number of elastically active junctions ($1/M_c^{NMR}$), whereas variations in the local structure of the networks (produced by use of different cure systems) only produce negligible effects.

Contrary to this observation, filled compounds follow two different scenarios, i.e., when there are or are no elastomer−filler interactions. To highlight this point, we focus on two of the rubber compounds, NR and SBR, both filled with pristine silica and with TESPT-modified silica (samples 7 and 11 for NR in Figure 3A and samples 6 and 9 for SBR in Figure 3B).

i. Pristine Silica: A Weakly Interacting Filler. The addition of silica to both NR and SBR leads to significant changes in the cross-link density, as it is indicated by the significant decrease of $1/M_c$ measured by NMR (vertical shifts in Figure 3). It confirms the general influence of the filler surface on the cure system, reducing its efficiency by mere adsorption of reactive species, e.g., vulcanization additives (such as MBTS) tend to adsorb on the silica surface, thus becoming inactive in the vulcanization,[95,96] or possibly involving specific effects of the hydroxyl groups present on the silica surface. Such effects are particularly strong when pristine silica is used; see the symbols 7 and 6 in Figure 3, parts A and B, respectively, as compared to their unfilled counterparts (denoted 3 in each plot). When these results are compared to the situation with silanization at the same level of filling (symbols 11 and 9 in Figures 3, parts A and B, respectively), it is clear that untreated silica has much weaker interactions with the rubber matrix, not restricting the swelling as much.

Such behavior is explained by reduced or completely missing interactions between elastomer chains and the silica surface in the swollen state. If this statement is true, eq 1 should not be applicable as it does not consider the excess of solvent present in the free space (vacuole) present at the interface of noninteracting composites[76] (it would assume $1/\phi_r^{fil} = V_{fil} = V_{fil}^{net} + V_{fil}^{int}$). Hence, eq 2 should be used to properly calculate the volumetric fraction of rubber via swelling experiments,[75] which correctly yields $1/\phi_r^{fil} = V_{fil}^{net} = V_{fil} - V_{fil}^{int}$ for use in the Flory−Rehner equation, where V_{fil} defines the total volume of solvent present in the filled sample, V_{fil}^{net} is the solvent that is actually swelling the elastomer network, and V_{fil}^{int} stands for the solvent volume located in the interface.

It is important to note that the osmotic expansion of the polymer matrix exerts a strong force on the polymer that may

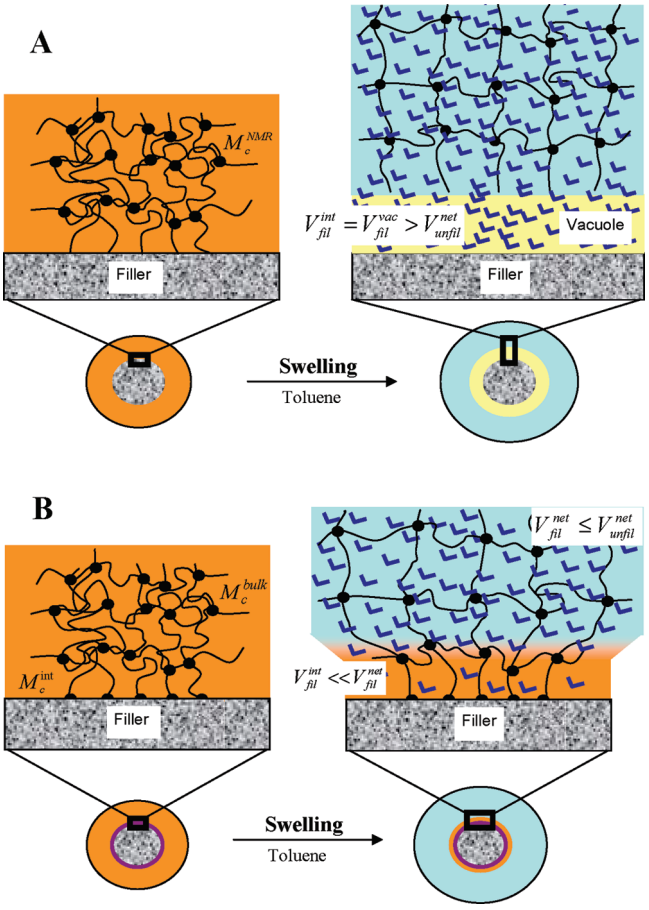

Figure 5. Schematic comparison of the swelling behavior of an elastomer composite without interactions between filler particles and the rubber matrix (A) and a composite with filler−rubber interactions (B).

be adhering to the filler surface. This process thus favors the polymer debonding from the filler surface even in the case when solvent−polymer interactions are more favorable than the solvent−filler interactions.

The presence of vacuoles around the filler particles is independently confirmed by cryoporosimetry measurements (Figure 4). All samples show two well-defined endothermic peaks attributed to the solvent present inside (peak 1, lower melting temperature) and outside (peak 2, higher melting temperature) the rubber matrix. Peak 2 corresponds to the melting of the solvent excess that is in the DSC pan but is not swelling the rubber matrix. Slight differences in the melting temperature could be explained by colligative effects. In addition, variations in intensity are only caused by the different excess of solvent in each sample.

The substantial low-temperature shift of peak 1 in the unfilled sample is caused by the small mesh size of the polymer network. While the use of silanized silica yields a network that swells overall less and shifts peak 1 toward low temperature, addition of pristine silica shifts peak 1 to higher temperature because of a dramatic decrease in the size restrictions—a considerable amount of frozen solvent is now present in larger vacuoles, in effect shifting the maximum. Figure 5A shows a schematic picture of the assumed scenario.

When we implement the correction (using eq 2 rather than eq 1 to calculate ϕ_r), we, in fact, obtain an increased deviation from the masterline (unfilled vs filled symbols). The direction of the correction is reasonable. With the presence of vacuoles, less solvent participates in the actual network swelling; thus, the true ϕ_r is smaller than the one given by eq 1. However, the now increased deviation from the masterline shows that also in these unsilanized but highly filled compounds there are some filler−elastomer interactions that restrict the swelling somewhat. Nevertheless, the deviation from the masterline is still much smaller than for systems with the same amount of active, silanized filler. This behavior may be explained by larger scale inhomogeneities in the swollen system, possibly due to a mechanical mesh of filler particles that are "glued" together. Such large and irregularly shaped aggregate structures may not allow for an affine expansion of the rubber matrix around it. In other words, strong and solvent-resistant filler networking may also contribute to restrictions on swelling.

ii. TESPT-Modified Silica: A Strongly Interacting Filler. A different situation is observed in samples filled with silane-modified silica, e.g., number 11 and 9 for NR and SBR in Figure 3, parts A and B, respectively, as already noted above. TESPT is a bifunctional organosilane widely used in rubber science and technology. On one hand, it is grafted onto the silica surface by the reaction of the ethoxy groups of the silane molecules with the hydroxyl groups present on the silica surface. On the other hand, the sulfane functionality can participate in the vulcanization process, creating covalent bonds with the elastomer chains. In consequence, variations in the vulcanization efficiency caused by the presence of silica hydroxyl groups are not probable; to the contrary, the formation of extra cross-links at the filler−rubber interface is expected.

The negligible vertical shift of these compounds with respect to the corresponding unfilled samples in Figure 3, as well as the absence of broadening of D_{res} distribution (Figure 1B), indicates that our NMR experiments are in this case insensitive to filler−rubber interactions, in accordance with the previously published results in SBR.[62] This merely means that the (undoubtedly present) silica−polymer cross-links are much closer on average than the cross-links in the bulk ($M_c^{int} \approx M_c^{bulk}$) or that a region of increased cross-link density close to the filler contributes only a small volume fraction as compared to the overall amount of rubber matrix. The situation would only change for well-dispersed nanometric fillers with large grafting density, for which the NMR-detected cross-link density is expected to be increased as well as spatially inhomogeneous. Such a behavior is indeed observed in recent experiments on model-filled ethyl acrylate elastomers, which will be published soon.

We should mention that recent works on filled poly(dimethylsiloxane) networks (PDMS) do show a certain increase of the average residual dipolar couplings (related to the number of constrains) upon addition of interacting fillers using MQ ^{1}H NMR experiments.[63,64] In the case of silica−PDMS composites, this increase of D_{res} is not surprising because, albeit being overall unpolar, PDMS forms strong hydrogen bonds with hydroxyl groups on the silica surface (due to its local dipoles). These interactions lead to the formation of a glassy layer; consequently, pristine silica particles in PDMS behave as giant cross-links, which are further much better dispersible than in incompatible polymers such as NR and SBR. In conclusion, untreated silica is considered an active bound filler for PDMS but inactive in the case of nonpolar rubber like SBR.

Although $1/M_c$ seems to be invariant, swelling measurements reveal a clear deviation from the masterline (horizontal shifting) when silanized silica is dispersed into the elastomer, $V_{fil} < V_{unf}$. In consequence, the reduction of swelling capacity of these samples (number 11 and 9 in NR and SBR compounds represented in Figure 3, parts A and B,

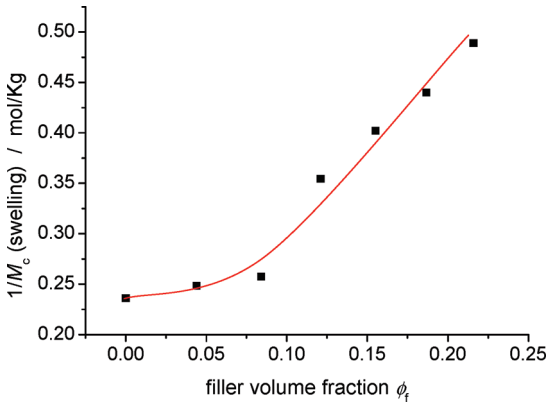

Figure 6. Variation of the apparent cross-link density of NR3 compounds filled with TESPT-modified silica as a function of filler volume fraction. These data were extracted from Figure 3A for a clearer presentation. The line is only a guide to the eye.

respectively) must be related to the different swelling behavior within the filler−rubber interface, $V_{fil}^{int} < V_{fil}^{net} \leq V_{unfil}$. Figure 5B shows a schematic picture of the assumed scenario to explain the swelling behavior of filled compounds with filler−rubber interactions, which is the key of this article.

Fillers are unswellable particles that contain some elastomer chains connected to their surface; hence, fillers behave like macro cross-links. In consequence, the swelling behavior of rubber connected to the filler surface is strongly limited in comparison to the bulk behavior (independently of whether M_c^{int} is or is not different from M_c^{bulk}). The total volume of solvent measured in equilibrium swelling experiments is the sum of two contributions: the fraction of solvent in the interface and the solvent that is swelling the bulk. According to the described statement, significant deviations from the masterline are expected and demonstrated experimentally (Figure 3).

Within this scenario, one would expect a very broad distribution of apparent residual dipolar couplings in the swollen state, as the network close to the filler swells much less than the rest. In consequence, an inhomogeneous strain field could be assumed.[76] Unfortunately, it is not possible to detect this by MQ NMR experiments because the previously demonstrated heterogeneous nature of swelling process itself masks this gradient[90−92] (data do not shown).

It is important to consider the influence of the interface on the bulk behavior, which is also reflected in the cryoporosimetry results, as can be seen in Figure 4. The interface created by the covalent filler−rubber interactions leads to increased restrictions. In consequence, freezing of the solvent primarily takes place in the less restricted network bulk rather than in the interface. Figure 4 shows that the melting point of the solvent that is swelling the rubber network is depressed in comparison to the unfilled sample. Taking into consideration that both samples have practically the same cross-link density as measured by NMR, hence the same mesh size, the only explanation is the decrease of swelling capacity of the bulk network because of the presence of filler particles and the influence of the interface. Similar results were obtained by measuring the freezing point depression of SBR composites (see legend of Figure 3B).

iii. Influence of Filler Volume Fraction and Filler Networking. The filler volume fraction in compounds with interacting particles becomes a very important parameter. This is obvious from Figure 6, where we see that the addition of 10−20 phr TESPT-modified silica leads to almost negligible changes in the apparent $1/M_c$ (i.e., almost invariant swelling behavior). However, a nonlinear behavior, with a marked increase in swelling restrictions, is observed in samples filled with 30 phr or more of modified silica. According to the NMR results, a slight decrease of $1/M_c$ is observed as the filler fraction increases, which may be due to an adsorption of a part of the vulcanization ingredients, as already mentioned above. Nevertheless, neglecting this tiny variation of the *true* cross-link density among these samples, the small deviation of lowly filled composites with respect to the masterline, even with proven filler−rubber interaction, is easily explained by a low fraction of rubber in the interphase, $V_{fil} \approx V_{fil}^{net} \approx V_{unfil}$ (see Figure 5). The effective cross-link density measured in the swelling experiments should be related to the elasticity modulus of the samples, and previous work has shown that the latter is a nonlinear function of the filler volume fraction ϕ_f.[49] The increased apparent cross-link density observed for the composites with 30 phr or more of modified silica (corresponding to volumetric fractions $>12\%$) is obviously not proportional to the increase of rubber present in the interface. It was demonstrated in the literature that a percolated filler network is formed at similar volume fraction of fillers.[97,98] Therefore, we hypothesize that filler percolation may also explain the nonlinear correlation shown in Figure 6. Only geometrical effects have to be considered here because the solvent would plasticize the possible glassy layers. At low/moderate volume fraction of filler, rubber at the interface merely increases the effective filler volume fraction. At higher filler volume fraction, above the percolation threshold, the interfaces overlap and the system enters a strongly reinforcing regime, in which many filler particles are tightly linked and form even larger effective cross-links, explaining the nonproportional reduction of solvent volume in the composites. In conclusion, the deviations from the masterline, and also the actual reinforcement of the elastomer matrix, are largely due to the formation of a continuous filler network. Detailed mechanical investigations supporting this issue were performed and are the subject of a subsequent publication.

The results obtained for SBR shown in Figure 3B suggest a less dramatic nonlinear behavior upon going from samples with 10 and 20 phr of TESPT-modified silica to about 40 phr. We point out that filler percolation phenomena and the ultimate reinforcement are also dependent on the primary aggregation and agglomeration state of the filler, indicating that future work must also include scattering studies characterizing the filler network structure. Analogous behavior is observed in NR samples filled with carbon black (samples 6 and 13 in Figure 3A). Although there is no evidence of significant variation in both the average M_c and its distribution detected by NMR (see Figure 1B), there are again significant variations in the swelling capacity. Following the same reasoning as above, we assume that the described behavior may be again related with the formation of a percolated filler network somewhere between 16 and 45 phr of carbon black, in agreement with the results obtained by other techniques.[97,98]

In consequence, the filler network seems to be a main factor determining the improvement of mechanical properties and the restrictions on the swelling capacity of filled elastomer compounds. Individual interacting filler particles are big multifunctional cross-links, whose effective size increases further when they become mechanically connected upon filler network formation. In this sense, a further increase of the swelling degree (a decrease in the restrictions to swelling) at longer times could be expected at least for carbon black composites, for which physical absorption is more dominant than chemical bond formation, as the swelling

stress and the solvent action may break down the physical filler−filler bonds (created thought glassy layers). This supposition is analogous to the bound-rubber determination by solvent extraction, which is known to be time dependent, and will be tested in the future.

iv. Influence of the Strength of the Filler−Matrix Interaction. Another important parameter to tune and understand the reinforcement of filler compounds is the actual nature of the filler−matrix interaction.[51] The first example was already given by the comparison of NR and SBR filled with carbon black and TESPT-modified silica (samples 5 and 6 for NR in Figure 3A and samples 4 and 5 for SBR in Figure 3B). These samples contain the same filler volume fraction and were prepared and processed under the same conditions, yet the silica-filled compounds seem to have stronger swelling restrictions, and hence larger deviations from the masterline, than the carbon black compounds. Since both composites do not show any remarkable variation in the overall cross-link density and its heterogeneity with respect their unfilled counterpart (see Figure 1B), differences in swelling are related to the different nature and strength of the filler−elastomer interactions (physical absorption vs chemical bonds) and also to differences in the filler network structure (aggregation).

Considering that a proper separation of effects of aggregate and agglomerate structure without dedicated scattering experiments is not possible, a cleaner indication of the importance of the filler−matrix interaction strength may be gleaned from changing just the nature of the silane coupling agent in composites filled with pretreated silica. Although different silanes may have some influence on filler dispersion upon compounding, we consider that the main factor that determines the observed differences in these samples should be attributed to the strength of the filler−matrix interaction.

Figure 7 shows the effect of three different silane modifications in both NR and SBR composites. First of all, it is important to point out again that all unfilled samples follow the masterline. Differences in the cross-link density of these samples (vertical shifts) are caused by the influence of the different silane molecules on the overall vulcanization reaction (see samples NR3-u, NR3-u-A, NR3-u-B, NR3-u-C, and their SBR counterparts in Figure 7). As already mentioned above, pristine silica (sample NR3-40S) decreases the cross-link density because of partial adsorption of vulcanization accelerators. Then, independently of the type of silane molecule used to modify the silica surface, the modification produces both an increase in cross-link density and a decrease in the swelling capacity (horizontal shift) with respect to the pristine silica. TESPT appears to be the most effective silane, as it leads to the strongest effects in both NR and SBR composites, followed by MS silane and NXT. These results could be related to the different reactive groups of these molecules. The TESPT molecule contains a distribution of polysulfur bridges (mean at $-S_3-/-S_4-$), and MS silane contains a mercapto function (−SH); the cross-link density is modified at the interface with more dissipative bonds in the case of TESPT. TESPT results in a more complex cross-link network around the filler than MS or NXT silanes, which give a simple link (reactivity of a mercapto function with an ethylenic double bond).

Independently of the reasons to improve the strength of the filler−matrix interaction, it is thus demonstrated that the effect of the interfacial interactions is observed to be qualitatively equivalent to the influence of filler volume fraction on the swelling restrictions, and therefore it is of similar importance for the rubber reinforcement.

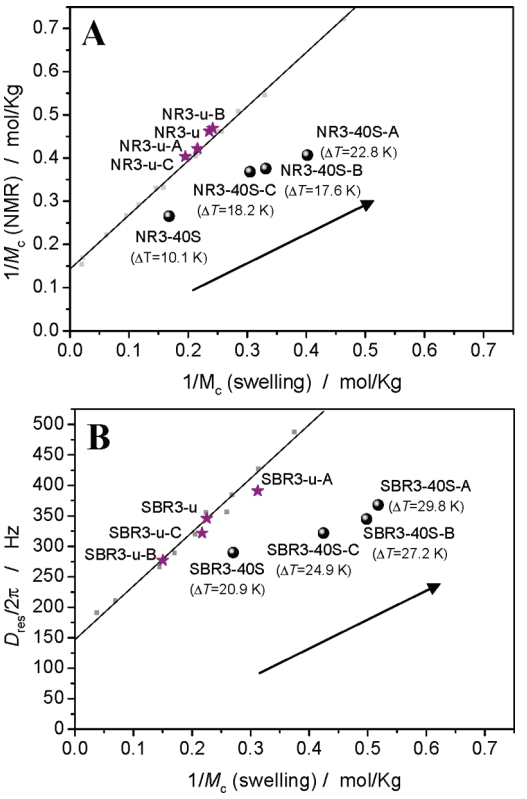

Figure 7. Deviation of the swelling capacity of NR (A) and SBR (B) compounds filled with different silane-modified silica particles with respect to their respective masterlines. The arrow indicates the increasing strength of the filler−matrix interaction according to the different silanes used in the silica modification. Values in parentheses are the freezing point depressions of cyclohexane imbibed in the elastomer samples.

Although samples described in this section appear to exhibit a correlated behavior, this apparent correlation disappears when different types of filled samples are represented together. In order to explain this phenomenon, one has to keep in mind that the relationship between the actual $1/M_c$ and the swelling restrictions in silica-filled composites is influenced by two different factors: (i) the different effect of silane molecules on the efficiency of the vulcanization reaction (vertical shift in Figure 7) and (ii) the different strength of the filler−rubber interactions caused by the nature of the silane molecules (horizontal shift in Figure 7). Both effects reduce the swelling capacity of rubber compounds. In consequence, a larger depression of the solvent freezing point was observed (see Figure 7).

2. Elastomer Nanocomposites. Nanocomposites are a new paradigm in the field of elastomer materials because of their high-performance properties with a significant reduction in weight. The impressive possibilities of these materials are based on the nanosize and high aspect ratio that characterize the nanoparticles. As was mentioned in the Introduction, nanocomposites have a low percolation threshold and extensive interfacial area per volume of particles, which are the main factors enhancing the formation of strong interphases. In consequence, the interphase volume is very important in nanocomposites, as it is possible that it percolates though the entire material at very low volume fraction, thus dominating the entire bulk. Combination of NMR and swelling experiments is an excellent experimental approach to check whether the *nanoeffect* on elastomer properties is caused by these interfacial phenomena.

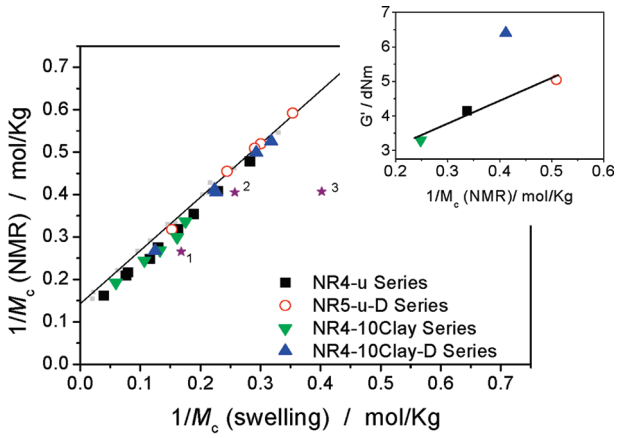

Figure 8. Swelling capacity of NR−clay nanocomposites in comparison with their unfilled counterparts. Each series contains samples vulcanized with different sulfur content. As a reference, samples NR3-40S, NR3-20S-A, and NR3-40S-A are also represented as 1, 2, and 3, respectively. The inset shows the modulus corresponding to samples vulcanized with 2.5 phr sulfur; the line is only a guide to the eye.

i. Elastomer−Clay Nanocomposites. Elastomer−clay nanocomposites are probably the most widely studied system in the field of rubber nanocomposites. Significant improvements of properties without reduction in elasticity with respect to unfilled systems or microcomposites are only realized if an exfoliated structure is obtained. Nonpolar rubbers are not able to penetrate the clay platelets, and consequently, microcomposites are obtained without any benefit over conventional fillers. We here use montmorillonite that was modified with octadecylamine by an ion exchange reaction.[27] Intercalation of the amine molecules increases the interlayer spacing and facilitates the clay exfoliation in NR nanocomposites. It leads to significant improvements of mechanical properties of around 350% over NR composites filled with the same amount (10 phr) of carbon black, being equivalent in properties to those composites obtained by the addition of as much as 40 phr of carbon black.[27]

We should point out that these samples were prepared from a different batch of NR. Their swelling behavior was evaluated previously,[27] and the NMR analysis was also performed back then; however, the corresponding results were not yet published. For this work, these earlier results were revised with regards to the multiple corrections for the swelling data that we have found to be significant in the meantime.[75] This could explain the small and insignificant deviations from the figures given in ref 27. Note that due to the relatively low filler levels, the correction described by eq 2 over eq 1, taking solvent vacuoles into account, is negligible. The different sample batch and different processing conditions may explain why these data are not exactly on the masterline, as also commented earlier.[75]

NMR analysis indicates that the addition of 10 phr of pristine montmorillonite (NR4-10Clay) varies the mesh size of the elastomer network, yet without significant change in the homogeneity of the cross-link distribution in comparison with its unfilled counterpart (Figure 1C). This already indicates that a significant "nano" effect on the cross-link density in the interphase is not detectable (understanding this term as particle−rubber interactions able to create some interfacial phenomena that dominate the entire bulk). In addition, the most important observation is that equilibrium swelling experiments do not reveal any significant deviation from the masterline (Figure 8). This result clearly reveals that clay particles do not significantly interact with the rubber matrix, no matter whether they are dispersed/exfoliated or not.

The only significant change we observe is that the overall cross-link density varies substantially between the different series, as also indicated by the shift of the average value of D_{res} in Figure 1C or the equivalent changes in Figure 8. While at a given sulfur content, addition of pure clay decreases the cross-link density (indicating the usual filler−surface related absorption effects, decreasing the vulcanization efficiency), the addition of organoclay leads to a substantial increase in cross-link density, however only along the masterline, indicating that the whole rubber matrix rather than an interphase region is affected. The origin of this effect is highlighted by the series containing only the octadecylamine but no clay (series NR5-u-D), which shows the largest increase. This is not unexpected, as amines act as accelerators, simply increasing the efficiency of the cure system. As compared to this series as the *proper* reference, the organoclay samples are in fact *inferior*, indicating also here again no interaction with the polymer chains, but rather a decrease in efficiency of the vulcanization reaction, as the exfoliated clay surface effectively immobilizes/binds parts of the amine (accelerator).

Therefore, while the large non-interacting inner surface might well lead to local changes in the glass transition of the polymer (in agreement with ample thin-film work), there is no discernible nanofiller effect on the elasticity of the polymer matrix, as unambiguously detected by NMR. Once the desired *nano*effect has been discarded, it is of course important to clarify why other macroscopic properties of these samples are much improved. The inset of Figure 8 shows the elastic modulus (measured as shear modulus with a constant strain of 6.96% and frequency of 1.667 Hz) of four samples with identical sulfur content as compared to the NMR-determined cross-link density. While three of the samples follow the expected linear dependence between cross-link density and modulus, only the exfoliated sample deviates substantially. In consequence, it is possible to identify the mechanical filler network as the major origin of the reinforcement behavior. On the side, it is important to take into consideration that the final properties beyond the linear regime of mechanical response are considerably affected by some other factors outside the scope of this work, such as strain-induced crystallization.

We conclude that the comparison of NMR and swelling experiments directly proves that substantial reinforcement effects in rubber−clay nanocomposites (i) can be achieved without chemical or physical bonds between polymer and filler and (ii) are mainly due to geometric effect of stiff and well-dispersed filler platelets. In other words, the reinforcement mainly benefits from the increased modulus of the percolated mechanical network[32] as compared to the soft matrix. This straightforwardly explains why the exfoliated rubber composites do show significantly enhanced mechanical properties, while the "nanoeffect" falls short of the expectations for harder polymer matrices.[32]

ii. Graphene−Elastomer Nanocomposites. While clay nanocomposites have started to appear in large quantities in consumer products, carbon-based nanofillers are a promising alternative. Carbon nanotubes (SWNTs) have become a key player in the field because they lead to improvements in mechanical properties, along with exceptional electrical conductivity, thermal conductivity, thermal stability, and low flammability.[31] However, their high price poses strong limitations on their large-scale use, and other restrictions are set by the difficult control of the agglomeration of the

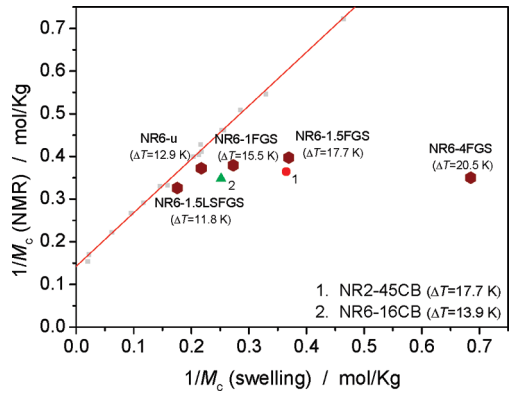

Figure 9. Deviation of the swelling capacity of NR−graphene nanocomposites from the unfilled NR masterline. Values in parentheses indicate the freezing point depression of cyclohexane imbibed in the elastomer samples.

individual nanotubes into low-modulus bundles that control the mechanical stability and strength of the SWNT−polymer nanocomposites.[31,32,99]

Recently, graphene-based fillers, such as functionalized graphene sheets (FGS), also termed thermally expanded graphite oxide (TEGO) vitalized the field as they offer similar properties as SWNTs, combined with other advantageous properties of the cheaper natural clays.[77,100−102] FGS is obtained by thermal expansion of graphite oxides,[77,78,103] producing a high-surface-area carbon material (600−800 m^2 g^{-1} from N_2 BET and 1850 m^2 g^{-1} from methylene blue adsorption in ethanol), consisting of single wrinkled sheets of partially oxidized graphene.[77,78,103]

According to the NMR results, NR−FGS nanocomposites do not show any substantial variation in the cross-link density with respect to their unfilled counterpart, as is apparent from Figure 1D and the lack of vertical shift in Figure 9. Other network parameters such as the spatial homogeneity of the cross-link density (see also Figure 1D) or the amount of nonelastic network defects (data not shown) also do not change substantially upon addition of FGS. As the FGS is known to be almost fully dispersed,[77] these compounds can be expected to exhibit the largest volume fraction of "interphase material", and we can here conclude that its NMR properties do not differ much from the overall rubber matrix. Therefore, rubber−filler bonds, if present, are not much denser than the bulk cross-links. (Otherwise, substantially broadened D_{res} distributions would result, as we have seen in model-filled compounds with nanosized fillers with high grafting density.) Note that we carefully calibrated and checked the integrated proton NMR signal per sample weight, confirming that no substantial amounts (< 1%) of rubber material are "invisible" (broadened beyond detection) due to potential paramagnetic centers on the filler surface.

Nevertheless, the addition of just a few percent of these carbon-based nanoparticles leads to an impressive horizontal shift in the swelling behavior shown in Figure 9, suggesting that in the swollen state the material properties are completely dominated by the interface behavior, revealing a significant *nano*effect. For example, 1% of FGS nanocomposite shows higher swelling restrictions than the NR composite containing 16 phr of carbon black. Addition of 1.5% of FGS is equivalent to the effect of 45 phr of carbon black, while the swelling restrictions imposed by 4% of FGS are completely beyond the range investigated so far. Freezing point depression measurements of cyclohexane imbibed in these elastomer nanocomposites (also shown in Figure 8) are in line with these observations.

The large effects observed here and, in consequence, the superior reinforcing effect of FGS are thus related to two factors: the wrinkled nanoscale topology and the high polymer-accessible surface area. As was demonstrated,[103,104] distortions caused by oxygen functionalization in the graphite oxide precursor and the resulting defects during thermal exfoliation, as well as the atomic-scale thickness of the resulting sheets, lead to a wrinkled topology. The resulting surface roughness enhances a mechanical interlocking with the polymer chains (similar to the effect of carbon black but on a more well-defined nanoscale), and in consequence, improved adhesion is obtained. The high accessible surface area is another key factor. Figure 9 also shows a comparison between two similar compounds with 1.5% FGS; the only difference is the nanoparticle surface area. While high-surface-area FGS shows a very significant deviation from the masterline, its low-surface-area counterpart does not significantly differ from its unfilled compound.

Finally, it is important to point out that the variation of the solvent fraction in the swollen samples (i.e., their equilibrium degree of swelling) is roughly proportional to the volume fraction of nanofiller, while silica-filled compounds exhibit a nonlinear correlation that is possibly due to a particle percolation phenomenon. In conclusion, by comparing both sample series, one may assume that even the smallest amount of FGS leads to a percolated filler network. This is in fact corroborated by the fact that all investigated FGS composites are electrically conductive.[77]

Conclusions

Reinforcement of elastomers is a central topic in rubber science and technology. The addition of fillers and nanofillers affect the matrix properties mainly because of the creation of an interface, at which the elastomer has a different behavior than in the bulk. Characteristics of the interphase material are related to other factors, such as the elastomer−particle interactions (nature, strength, ...), the filler volume fraction, the filler dispersion, or the filler networking. The lack of experimental techniques yielding information on the elastomer−particle interactions represents a serious obstacle for progress in designing new improved materials. Therefore, our combination of solid-state ^{1}H low-field MQ NMR spectroscopy and equilibrium swelling experiments represents an important step forward.

While it is common practice to correlate the creation of filler−elastomer interactions, i.e., strong and glassy interfaces, with the increased cross-link density measured by the equilibrium swelling experiments or with enhanced mechanical properties, no direct information can be gained on the *actual* number of elastically active junctions (comprising cross-links and rubber−filler bonds) that affect the elasticity of the elastomer matrix. As we have shown herein, dramatic changes in macroscopic properties such as the degree of swelling are possible, while the matrix properties are either unaffected or even deteriorated. It stresses the importance of a molecular approach for M_c determination such as NMR in general, and of MQ NMR experiments in particular, as they were previously demonstrated to not be subject to filler-induced artifacts.

In unfilled elastomers, linear relationships are obtained when swelling results are compared with the NMR observable because the degree of swelling measures rubber elasticity in terms of the average $1/M_c$ directly. Therefore, deviations from this masterline in filled systems immediately identify filler-induced effects that are beyond changes in the overall matrix elasticity.

We have observed two different scenarios, where, on the one hand, without rubber−filler interactions solvent-filled vacuoles form around the fillers and no deviation from the masterline is observed. On the other hand, the formation of strong rubber−filler bonds leads to a reduction of the swelling capacity because the nonswellable filler particles then act as giant cross-links, creating an inhomogeneous strain field around the particles in the swollen network. The so-identified filler effects are among those that are responsible for the improvements in mechanical properties beyond the simple hydrodynamic effect, depending on the interfacial characteristics including a potential glassy layer, the effective filler volume fraction, its dispersion, and aggregation state.

As the most exciting class of materials, nanocomposites of NR with functionalized graphene sheets (FGS), with its wrinkled and flexible "2D polymer" nanoscale topology and large interfacial area, were found to exhibit huge effects on the swelling capacity of the samples that are in line with their significantly improved mechanical properties, however without any significant changes in the cross-link density of the rubber matrix. This should be contrasted with the popular elastomer−clay nanocomposites, which also do not show any filler-specific changes in the NMR-determined cross-link density but also, and more surprisingly, no indication of significant matrix−filler interaction as well. On the other hand, exfoliated clay composites do show significantly enhanced mechanical properties, which are thus explained to be due to filler−filler interactions only, possibly just the hard-body repulsion of stiff platelets. This comparison stresses the importance of functionalized graphene sheets as a qualitatively new type of nanofiller in rubber science.

The application of the novel experimental approach presented in this article is expected to contribute to improved insight into the not well understood structure−property relationships in filled-rubber science.

Acknowledgment. J.L.V. thanks the Alexander von Humboldt Foundation as well as the Ministerio de Educación y Ciencia (Spain) for his fellowships. Financial support from CICYT (MAT 2008-1073) is also gratefully acknowledged. K.S. thanks the DFG (SFB 418) and the European Union (ERDF programme) for financial support. We thank Dr. Ing. Laurent Guy (Rhodia) for providing the NR1,2 and SBR1,2 sample series and for fruitful discussions. We further thank Prof. R. K. Prud'homme (Department of Chemical Engineering, Princeton University) for supplying the NR6 samples filled with FGS analyzed in this article.

Supporting Information Available: Detailed descriptions of sample recipes and preparation procedures. This material is available free of charge via the Internet at http://pubs.acs.org.

References and Notes

(1) Kraus, G. *Reinforcement of Elastomers*; Interscience: New York, 1965.
(2) Allen, P. W.; Lindley, P. B.; Payne, A. R. *Use of Rubber in Engineering*; Maclaren and Sons Ltd.: London, England, 1966.
(3) Freakley, P. K.; Payne, A. R. *Theory and Practice of Engineering with Rubber*; Applied Science Publishers Ltd.: London, England, 1978.
(4) Mark, J. E.; Erman, B.; Eirich, F. R. *Science and Technology of Rubber*, 2nd ed.; Academic Press: San Diego, CA, 1994.
(5) Donnet, J.-B.; Bansal, R. C.; Wang, M.-J. *Carbon Black: Carbon Black: Science and Technology*, 2nd ed.; CRC Press: Boca Raton, FL, 1993.
(6) Medalia, A. I. *Rubber Chem. Technol.* **1978**, *51*, 437–523.
(7) Rigbi, Z. *Adv. Polym. Sci.* **1980**, *36*, 21–68.
(8) Klüppel, M.; Schuster, R. H.; Heinrich, G. *Rubber Chem. Technol.* **1997**, *70*, 243–255.
(9) Heinrich, G.; Klüppel, M. *Adv. Polym. Sci.* **2002**, *160*, 1–44.
(10) Koga, T.; Hashimoto, T.; Takenaka, M.; Aizawa, K.; Amino, N.; Nakamura, M.; Yamaguchi, D.; Koizumi, S. *Macromolecules* **2008**, *41*, 453–464.
(11) Schröder, A.; Klüppel, M.; Schuster, R. H.; Heidberg, J. *Carbon* **2002**, *40*, 207–210.
(12) Wagner, M. P. *Rubber Chem. Technol.* **1976**, *49*, 703–774.
(13) Donnet, J.-B. *Rubber Chem. Technol.* **1998**, *71*, 323–341.
(14) Voet, A.; Morawski, J. C.; Donnet, J. B. *Rubber Chem. Technol.* **1977**, *50*, 342–355.
(15) Sun, C.-C.; Mark, J. E. *Polymer* **1989**, *30*, 104–106.
(16) Ikeda, Y.; Kohjiya, S. *Polymer* **1997**, *38*, 4417–4423.
(17) Wang, M.-J. *Rubber Chem. Technol.* **1998**, *71*, 520–589.
(18) Saalwächter, K.; Krause, M.; Gronski, W. *Chem. Mater.* **2004**, *16*, 4071–4079.
(19) Valentín, J. L.; López-Manchado, M. A.; Posadas, P.; Rodríguez, A.; Marcos-Fernández, A.; Ibarra, L. *J. Colloid Interface Sci.* **2006**, *298*, 794–804.
(20) Bokobza, L.; Garnaud, G.; Mark, J. E.; Jethmalani, J. M.; Seabolt, E. E.; Ford, W. T. *Chem. Mater.* **2002**, *14*, 162–167.
(21) Castellano, M.; Conzatti, L.; Costa, G.; Falqui, L.; Turturro, A.; Valenti, B.; Negroni, F. *Polymer* **2005**, *46*, 695–703.
(22) Joly, S.; Garnaud, G.; Ollitrault, R.; Bokobza, L.; Mark, J. E. *Chem. Mater.* **2002**, *14*, 4202–4208.
(23) Varghese, S.; Karger-Kocsis, J. *Polymer* **2003**, *44*, 4921–4927.
(24) Frogley, M. D.; Ravich, D.; Wagner, H. D. *Compos. Sci. Technol.* **2003**, *63*, 1647–1654.
(25) Bokobza, L. *Polymer* **2007**, *48*, 4907–4920.
(26) Arroyo, M.; López-Manchado, M. A.; Valentín, J. L.; Carretero, J. *Compos. Sci. Technol.* **2007**, *67*, 1330–1339.
(27) Arroyo, M.; Lopez-Manchado, M. A.; Herrero, B. *Polymer* **2003**, *44*, 2447–2453.
(28) Siliani, M.; López-Manchado, M. A.; Valentín, J. L.; Arroyo, M.; Marcos-Fernández, A.; Khayet, M.; Villaluenga, J. P. *J. Nanosci. Nanotechnol.* **2007**, *7*, 634–640.
(29) Vaia, R. A.; Wagner, H. D. *Mater. Today* **2004**, *7*, 32–37.
(30) Bockstaller, M. R.; Michiewicz, R. A.; Thomas, E. L. *Adv. Mater.* **2005**, *17*, 1331–1349.
(31) Moniruzzaman, M.; Winey, K. I. *Macromolecules* **2006**, *39*, 5194–5205.
(32) Schaefer, D. W.; Justice, R. S. *Macromolecules* **2007**, *40*, 8501–8517.
(33) Raos, G.; Moreno, M.; Elli, S. *Macromolecules* **2006**, *39*, 6744–6751.
(34) Struik, L. C. E. *Polymer* **1987**, *28*, 1521–1533.
(35) Putz, K. W.; Palmeri, M. J.; Cohn, R. B.; Andrews, R.; Brinson, L. C. *Macromolecules* **2008**, *41*, 6752–6756.
(36) Tsagaropoulos, G.; Eisenberg, A. *Macromolecules* **1995**, *28*, 396–398.
(37) Tsagaropoulos, G.; Eisenberg, A. *Macromolecules* **1995**, *28*, 6067–6077.
(38) Tsagaropoulos, G.; Kim, J.-S.; Eisenberg, A. *Macromolecules* **1996**, *29*, 2222–2228.
(39) Arrighi, V.; Higgins, J. S.; Burgess, A. N.; Floudas, G. *Polymer* **1998**, *39*, 6369–6376.
(40) Arrighi, V.; McEwen, I. J.; Qian, H.; Serrano Prieto, M. B. *Polymer* **2003**, *44*, 6259–6266.
(41) Keddie, J. L.; Jones, R. A. L.; Cory, R. A. *Europhys. Lett.* **1994**, *27*, 59–64.
(42) Hall, D. B.; Dhinojwala, A.; Torkelson, J. M. *Phys. Rev. Lett.* **1997**, *79*, 103–106.
(43) Long, D.; Lequeux, F. *Eur. Phys. J. E* **2001**, *4*, 371–387.
(44) Starr, F. W.; Schröder, T. B.; Glotzer, S. C. *Macromolecules* **2002**, *35*, 4481–4492.
(45) Sotta, P.; Long, D. *Eur. Phys. J. E* **2003**, *11*, 375–388.
(46) Merabia, S.; Sotta, P.; Long, D. *Eur. Phys. J. E* **2004**, *15*, 189–210.
(47) Berriot, J.; Lequeux, F.; Montes, H.; Monnerie, L.; Long, D.; Sotta, P. *J. Non-Cryst. Solids* **2002**, *307*, 719–724.
(48) Berriot, J.; Montes, H.; Lequeux, F.; Long, D.; Sotta, P. *Macromolecules* **2002**, *35*, 9756–9762.
(49) Berriot, J.; Montes, H.; Lequeux, F.; Long, D.; Sotta, P. *Europhys. Lett.* **2003**, *64*, 50–56.
(50) Montes, H.; Lequeux, F.; Berriot, J. *Macromolecules* **2003**, *36*, 8107–8118.
(51) Merabia, S.; Sotta, P.; Long, D. R. *Macromolecules* **2008**, *41*, 8252–8266.
(52) Bansal, A.; Yang, H.; Li, C.; Cho, K.; Benicewicz, B. C.; Kumar, S. K.; Schadler, L. S. *Nat. Mater.* **2005**, *4*, 693–698.

(53) Putz, K.; Krishnamoorti, R.; Green, P. F. *Polymer* **2007**, *6*, 278–282.
(54) López-Manchado, M. A.; Valentín, J. L.; Carretero, J.; Barroso, F.; Arroyo, M. *Eur. Polym. J.* **2007**, *43*, 4143–4150.
(55) Balazs, A. C.; Emrick, T.; Russell, T. P. *Science* **2006**, *314*, 1107–1110.
(56) Wagner, D.; Vaia, R. A. *Mater. Today* **2004**, *7*, 38–42.
(57) O'Brien, J.; Cashell, E.; Wardell, G. E.; McBrierty, V. J. *Macromolecules* **1976**, *9*, 653–660.
(58) Litvinov, V. M.; Steeman, P. A. M. *Macromolecules* **1999**, *32*, 8476–8490.
(59) ten Brinke, J. W.; Litvinov, V. M.; Wijnhoven, J. E. G. J.; Noordermeer, J. W. M. *Macromolecules* **2002**, *35*, 10026–10037.
(60) Berriot, J.; Martin, F.; Montes, H.; Monnerie, L.; Sotta, P. *Polymer* **2003**, *44*, 1437–1447.
(61) Luo, H.; Klüppel, M.; Schneider, H. *Macromolecules* **2004**, *37*, 8000–8009.
(62) Saalwächter, K.; Klüppel, M.; Luo, H.; Schneider, H. *Appl. Magn. Reson.* **2004**, *27*, 401–417.
(63) Lewicki, J. P.; Maxwell, R. S.; Patel, M.; Herberg, J. L.; Swain, A. C.; Liggat, J. J.; Pethrick, R. A. *Macromolecules* **2008**, *41*, 9179–9186.
(64) Serbescu, A.; Saalwächter, K. *Polymer* **2009**, *50*, 5434–5442.
(65) Litvinov, V. M. *Macromolecules* **2006**, *39*, 8727–8741.
(66) Callaghan, P. T.; Samulski, E. T. *Macromolecules* **1997**, *30*, 113–122.
(67) Fischer, E.; Grinberg, F.; Kimmich, R.; Hafner, S. J. *Chem. Phys.* **1998**, *109*, 846–854.
(68) Demco, D. E.; Hafner, S.; Fülber, C.; Graf, R.; Spiess, H. W. *J. Chem. Phys.* **1996**, *105*, 11285–11296.
(69) Saalwächter, K. *Prog. Nucl. Magn. Reson. Spectrosc.* **2007**, *51*, 1–35.
(70) Brereton, M. G. *Macromolecules* **1990**, *23*, 1119–1131.
(71) Saalwächter, K. *Macromolecules* **2005**, *38*, 1508–1512.
(72) Saalwächter, K.; Herrero, B.; López-Manchado, M. A. *Macromolecules* **2005**, *38*, 4040–4042.
(73) Saalwächter, K.; Klüppel, M.; Luo, H.; Schneider, H. *Appl. Magn. Reson.* **2004**, *27*, 401–417.
(74) Luo, H.; Klüppel, M.; Schneider, H. *Macromolecules* **2004**, *37*, 8000–8009.
(75) Valentín, J. L.; Carretero-González, J.; Mora-Barrantes, I.; Chassé, W.; Saalwächter, K. *Macromolecules* **2008**, *41*, 4717–4729.
(76) Berriot, J.; Lequeux, F.; Montes, H.; Pernot, H. *Polymer* **2002**, *43*, 6131–6138.
(77) Prud'homme, R. K.; Ozbas, B.; Aksay, I. A.; Register, R. A.; Adamson, D. H. Functional Graphene-Rubber Nanocomposites. World Patent WO 2008/045778 A1.
(78) McAllister, M. J.; Li, J.-L.; Adamson, D. H.; Schniepp, H. C.; Abdala, A. A.; Liu, J.; Herrera-Alonso, M.; Milius, D. L.; Car, R.; Prud'homme, R. K.; Aksay, I. A. *Chem. Mater.* **2007**, *19*, 4396–4404.
(79) McKenna, G. B.; Horkay, F. *Polymer* **1994**, *35*, 5737–5742.
(80) Horta, A.; Pastoriza, M. A. *Eur. Polym. J.* **2005**, *41*, 2793–2802.
(81) Horkay, F.; McKenna, G. B.; Deschamps, P.; Geissler, E. *Macromolecules* **2000**, *33*, 5215–5220.
(82) Kraus, G. *Rubber World* **1956**, *1*, 67.
(83) Saalwächter, K.; Ziegler, P.; Spyckerelle, O.; Haidar, B.; Vidal, A.; Sommer, J.-U. *J. Chem. Phys.* **2003**, *119*, 3468–3482.
(84) Saalwächter, K.; Sommer, J.-U. *Macromol. Rapid Commun.* **2007**, *28*, 1455–1465.
(85) Weese, J. *Comput. Phys. Commun.* **1992**, *69*, 99–111.
(86) Weese, J. *Comput. Phys. Commun.* **1993**, *77*, 429–440.
(87) Valentín, J. L.; Fernández-Torres, A.; Posadas, P.; Marcos-Fernández, A.; Rodríguez, A.; González, L. *J. Polym. Sci., Part B: Polym. Phys.* **2007**, *45*, 544–556.
(88) López-Manchado, M. A.; Valentín, J. L.; Herrero, B.; Arroyo, M. *Macromol. Rapid Commun.* **2004**, *25*, 1309–1313.
(89) Jackson, C. L.; McKenna, G. B. *Rubber Chem. Technol.* **1991**, *64*, 760–768.
(90) Sommer, J.-U.; Saalwachter, K. *Eur. Phys. J. E* **2005**, *18*, 167–182.
(91) Saalwachter, K.; Kleinschmidt, F.; Sommer, J.-U. *Macromolecules* **2004**, *37*, 8556–8568.
(92) Sommer, J.-U.; Chassé, W.; Valentín, J. L.; Saalwächter, K. *Phys. Rev. E* **2008**, *78*, 051803.
(93) Graessley, W. W. *Adv. Polym. Sci.* **1974**, *16*, 1–177.
(94) Abdel-Goad, M.; Pyckhout-Hintzen, W.; Kahle, S.; Allgaier, J.; Richter, D.; Fetters, L. J. *Macromolecules* **2004**, *37*, 8135–8144.
(95) Bomo, F. *Macromol. Chem., Macromol. Symp.* **1989**, *23*, 321–328.
(96) Ramier, J.; Chazeau, L.; Gauthier, C.; Guy, L.; Bouchereau, M. N. *Rubber Chem. Technol.* **2007**, *80*, 183−193.
(97) Bogoslovov, R. B.; Roland, C. M.; Ellis, A. R.; Randall, A. M.; Robertson, C. G. *Macromolecules* **2008**, *41*, 1289–1296.
(98) Kohjiya, S.; Kato, A.; Ikeda, Y. *Prog. Polym. Sci.* **2008**, *33*, 979–997.
(99) Ajayan, P. M.; Schadler, L. S.; Giannaris, C.; Rubio, A. *Adv. Mater.* **2000**, *12*, 750–753.
(100) Kotov, N. A. *Nature* **2006**, *442*, 254–255.
(101) Stankovich, S.; Dikin, D. A.; Dommett, G. H. B.; Kholhaas, K. M.; Zimney, E. J.; Stach, E. A.; Piner, R. D.; Nguyen, S. T.; Ruoff, R. S. *Nature* **2006**, *442*, 282–286.
(102) Ramanathan, T.; Abdala, A. A.; Stankovich, S.; Dikin, D. A.; Herrera-Alonso, M.; Piner, R. D.; Adamson, D. H.; Schniepp, H. C.; Chen, X.; Ruoff, R. S.; Nguyen, S. T.; Aksay, I. A.; Prud'homme, R. K.; Brinson, L. C. *Nat. Nanotechnol.* **2008**, *3*, 327–331.
(103) Schniepp, H. C.; Li, J.-L.; McAllister, M. J.; Sai, H.; Herrera-Alonson, M.; Adamson, D. H.; Prud'homme, R. K.; Car, R.; Seville, D. A.; Aksay, I. A. *J. Phys. Chem. B* **2006**, *110*, 8535–8539.
(104) Duplock, E. J.; Scheffler, M.; Lindan, P. J. D. *Phys. Rev. Lett.* **2004**, *92*, 225502.